Marine and Petroleum Geology 119 (2020) 104451

Contents lists available at ScienceDirect

Marine and Petroleum Geology

journal homepage: www.elsevier.com/locate/marpetgeo

Research paper

Reservoir alteration of crude oils in the Junggar Basin, northwest China: Insights from diamondoid indices

Wenmin Jiang, Yun Li*, Yongqiang Xiong

State Key Laboratory of Organic Geochemistry (SKLOG), Guangzhou Institute of Geochemistry, Chinese Academy of Sciences, Guangzhou, 510640, PR China

ARTICLE INFO

Keywords:
Diamondoid indices
Biodegradation
Water washing
Gas washing
Mixing oils

ABSTRACT

Reservoir alteration of crude oils is ubiquitous in petroleum reservoirs. Alteration can change the composition and physicochemical properties of crude oils, and complicate oil–source correlations and origin studies of crude oils. Thus, the identification and assessment of reservoir alteration could provide a better understanding of the formation and evolution of crude oils. In this study, the effects of reservoir alteration (e.g., biodegradation, gas washing, water washing, and mixing) on oils in the Junggar Basin, northwest China, were identified and assessed by combining diamondoid indices with other commonly studied crude oil properties. The results indicate that: (1) diamondoid indices can be used to evaluate the intensity of reservoir alteration on oils (e.g., slight biodegradation and water washing has no effect on diamondoids; moderate biodegradation and water washing can result in a marked increase in diamondoid concentrations; severe biodegradation and water washing significantly changes diamondoid concentration and isomerization ratios); (2) diamondoid indices can assist in determining the type of reservoir alteration of oils (e.g., condensate formed by gas washing has a lower diamondoid concentration than that generated by thermal cracking; differing from biodegradation and water washing, gas washing can affect diamondoid ratios; mixing can be identified by a combination of diamondoid concentrations and other parameters, such as API gravity and biomarker indices in oils). Therefore, diamondoids provide specific information as to the reservoir alteration of oils, which is useful in further understanding of the origin and evolution of crude oils in the Junggar Basin.

1. Introduction

The Junggar Basin is a multi-stage petroliferous basin in northwest China. Many oil and gas reservoirs have been discovered along the northwestern, eastern, and southern margins, and central part of the basin (Fig. 1), among which the northwest margin and central part of the basin are two major oil-producing areas. In addition to normal crude oils, heavy oils, condensates, and gases have also been found in different areas of the basin. The hydrocarbons have multiple sources (Clayton et al., 1997), a wide range of thermal maturities (relatively low-mature to over-mature; Jiang et al., 2019), and experienced variable reservoir alterations, including biodegradation (Zhang et al., 1988; Wang, 1994; Fu et al., 2005; Chang et al., 2018), secondary migration (Xiao et al., 2010; Xiang et al., 2015), and mixing (Chen et al., 2003, 2016c; Cao et al., 2006).

Reservoir alteration of crude oils (e.g., biodegradation, water washing, gas washing, and mixing) is common in petroleum reservoirs, and can change the composition and physicochemical characteristics of oils (Peters and Moldowan, 1993). The effects of reservoir alteration on oils need to be clarified to better understand the sources and origins of crude oils. Due to their strong resistance to thermal and biological degradation, diamondoid indices have been developed to evaluate the origin, thermal maturity, and biodegradation of oils (Chen et al., 1996; Grice et al., 2000; Schulz et al., 2001). Recently, diamondoid indices (e.g., absolute concentrations and ratios) have been used to assess the source and thermal maturity of oils in the Tarim Basin (Li et al., 2018) and Junggar Basin (Jiang et al., 2019). Although some reservoir alteration effects on diamondoid compositions in oils have been noted (Grice et al., 2000; Li et al., 2014, 2018), a detailed understanding of these effects is still lacking.The main aim of this study was to investigate the application of diamondoid indices in the identification and evaluation of reservoir alteration (e.g., biodegradation, water washing, gas washing, and mixing) on Junggar Basin oils. This was achieved by determining changes in diamondoid indices and other parameters (e.g., API gravity, $\delta^{13}C$ value of whole oil, and biomarker indices) in the oils.

* Corresponding author.
E-mail address: liyun@gig.ac.cn (Y. Li).

https://doi.org/10.1016/j.marpetgeo.2020.104451
Received 9 December 2019; Received in revised form 3 May 2020; Accepted 8 May 2020
Available online 11 May 2020

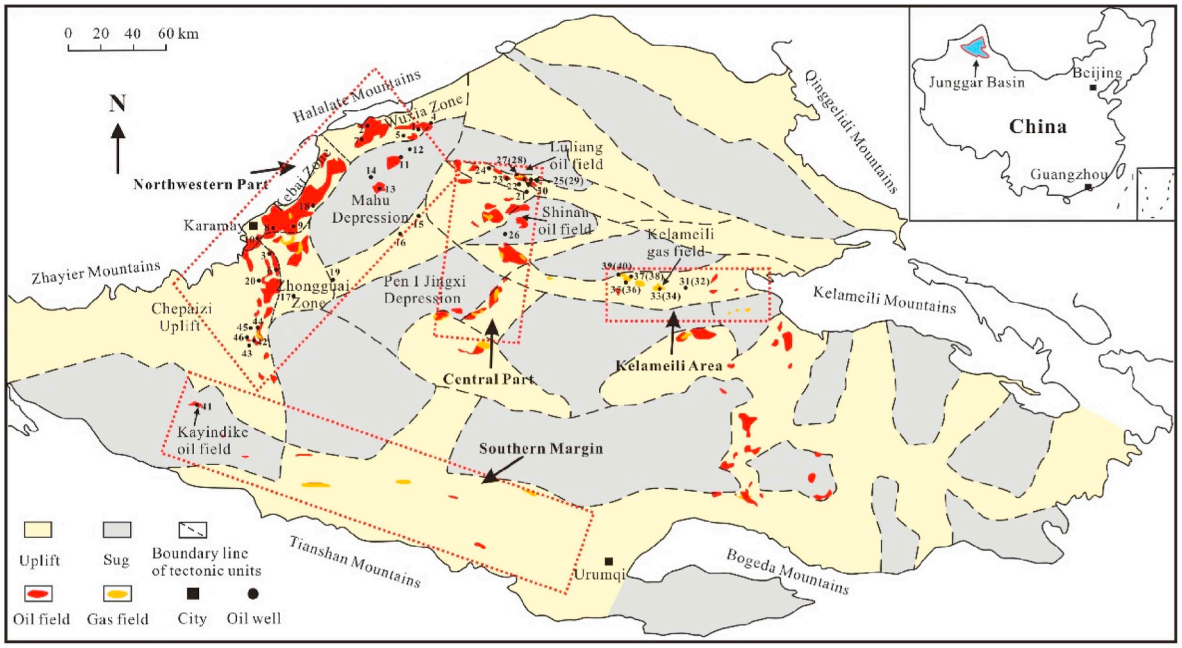

Fig. 1. Location map of the Junggar Basin, showing the sample locations.

2. Experimental methods

2.1. Sample preparation

The oil samples used in this study were collected from the Mahu Depression and Chepaizi Uplift in the northwestern Junggar Basin, the Kelameili area of the eastern Junggar Basin, the central Junggar Basin, and the southern margin of the Junggar Basin. Background information (e.g., location, API gravity, and $\delta^{13}C$ value of whole oil, etc.) regarding these oil samples is listed in Table 1. The samples include normal and heavy oils and condensates (Table 1).

The oil samples were firstly deasphaltened using excess hexane (40 × the oil volume). The maltene fraction was then separated into saturated, aromatic, and resin fractions in a silica gel column using hexane, hexane and dichloromethane (3:2 V/V), and methanol, respectively. Saturated and aromatic fractions were then concentrated and transferred into 4 mL sample vials for gas chromatographic (GC) and gas chromatographic mass spectrometry (GC − MS) analyses.

The samples for diamondoid determination were prepared using a simple solvent dilution method to avoid the evaporation of low molecular diamondoids during the preparation procedure. Approximately 50 mg of sample was added to a 4 mL glass vial filled with isooctane, after adding 100 μL of an internal standard solution, this sample solution was then ultrasonically treated for 10 min to improve the sample dissolution. Then the solution was centrifugated for 10 min to precipitate asphaltenes, and the supernatant was transferred to a 2 mL sample vial waiting for gas chromatography-triple quadrupole mass spectrometry (GC–MS–MS) analysis.

2.2. GC analysis

The GC analysis of the saturated fractions was conducted with an Agilent 7890A GC instrument equipped with a HP-5 column (30 m × 0.32 mm inner diameter × 0.25 μm film thickness) and flame ionization detector. The temperature of the GC oven was 60 °C for 2 min, ramped to 290 °C at 4 °C/min., and finally held for 30 min at 290 °C. Nitrogen was used as the carrier gas at a constant flow rate of 1.2 mL/min.

2.3. GC–MS analysis

The GC–MS analysis of the saturated and aromatic fractions was conducted on a Agilent 7890B GC coupled to a mass-selective detector (5977A), and equipped with a 30 m × 0.32 mm (inner diameter) HP-5 column with a film thickness of 0.25 μm. Helium was used as the carrier gas at a constant flow rate of 1.2 mL/min. The GC oven temperature was initially held at 80 °C for 2 min, ramped to 290 °C at 4 °C/min, and then held at 290 °C for 20 min. The mass spectrometer was operated in selected ion monitoring mode for the saturated fraction (*m/z* 191 for hopanes; *m/z* 217 for steranes) and in full scan mode for the aromatic fraction.

2.4. GC − MS − MS analysis

GC–MS–MS analysis was undertaken with a Thermo Fisher TSQ Quantum XLS instrument, and details of the analytical procedures are given by Liang et al. (2012). A 1 μL aliquot of each sample was injected into the GC system using an AS 3000 auto-sampler. The GC instrument was equipped with a PTV injector and a DB-1 fused silica capillary column (50 m × 0.32 mm inner diameter × 0.52 μm film thickness). These analyses used the PTV split-less mode with an inlet temperature of 300 °C, and a split flow of 15 mL/min following 1 min of split-less flow. Helium (99.999% purity) was used as the carrier gas at a constant flow rate of 1.5 mL/min. The GC oven temperature was initially set at 50 °C for 2 min, and then increased at 15 °C/min to 80 °C, 2.5 °C/min to 250 °C, and 15 °C/min to 300 °C, and was then held for 10 min at 300 °C. Quantification of diamondoid compounds was undertaken using a selected reaction monitoring (SRM) mode comparison between peak areas for the unknowns and two internal standards, which were *n*-dodecane-d_{26} for adamantanes and *n*-hexadecane-d_{34} for diamantanes.

3. Results and discussion

3.1. Biodegradation

Biodegradation of crude oils is a common phenomenon, and has been previously studied in the Junggar Basin (Wang, 1994; Fu et al.,

Table 1
Background date for the crude oil samples from the Junggar Basin.

Region	Zone/Oil field	No.	Sample name	Formation	Depth(m)	API gravity(°)	$\delta^{13}C$(‰)	PM rank[a]
Northwestern part	Mahu depression	1	X89	T_1b_2	2452–2474	35.3	−29.7	0
		2	W42	P_2w	1213–1258	29.9	−30.1	0
		3	H94	T_2k	1874–1892	28.9	−30.1	0
		4	X71	P_1f	4510–4530	31.1	−29.1	1
		5	X7202	T_1b_2	2754–2762	34.1	−28.8	1
		6	HS4	T_2k	1873–1876.5	33.2	−30.1	1
		7	W007	T_2k	1271–1256	27.0	−29.7	2
		8	HW5	T_2k	648–658	25.3	−29.3	2
		9	K129	C	479.5–484	24.2	−29.1	2
		10	HW8	T_2k	392–395	28.7	−30.2	3
		11	MA134	T_1b_2	3169–3188	42.0	−28.4	0
		12	MA15	T_1b_2	3048–3056	47.5	−28.0	0
		13	MA18	T_1b	3892–3920	40.7	−28.8	0
		14	MX1	T_1b	3582–3588	39.3	−28.8	0
		15	DA9	T_1b	4646–4727	43.5	−28.3	0
		16	DT1	C	5840–5864	46.0	−29.0	0
		17	XG1	P_1j	4552–4566	45.0	−29.6	0
		18	K901	C	1152–1172	35.4	−29.8	0
		19	G25	J_1s	2971–2979	34.9	−28.8	0
		20	HS6	C	1046–1086	34.6	−29.5	0
Central part	Shinan oil field	21	SN60	J_2x	2286–2291	33.4	−30.1	0
		22	SN62	J_2x_4	2148–2150.5	33.6	−30.0	0
	Luliang oil field	23	L11	J_2t	2072.5–2077	36.2	−30.2	0
		24	L12	J_2x	2038–2044	35.5	−29.8	1
		25	L27-2	J_2x	2138–2140.5	35.7	−29.5	1
	Shinan	26	SN42	K_1s	1536–1538	35.7	−29.0	1
	Luliang oil field	27	L9-1	K_1tg	1526–1528	33.2	−29.9	2
		28	L9-2	K_1tg	1579–1581	32.2	−30.0	2
		29	L27-1	K_1h	1686–1688	31.8	−29.0	3
		30	L103	K_1tg	1352–1356	30.3	−29.8	4
Eastern part	Kelameili gas field	31	DX21-1	C	2865–2876	46.4	−25.0	0
		32	DX21-2	C	2906–2913	47.9	−25.2	0
		33	DX10-1	T_3b	2695–2698	58.3	−25.3	0
		34	DX10-2	C	3024–3048	54.1	−25.4	0
		35	DX14-1	J_1b	2984–2989.5	57.2	−26.8	0
		36	DX14-2	P_3w	3523–3550	50.4	−26.8	0
		37	D403-1	C	3594–3606	55.5	−26.7	0
		38	D403-2	C	3824–3840	49.0	−27.1	0
		39	DX17-1	P_3w	3519–3526	59.5	−27.8	0
		40	DX17-2	C	3662–3670	51.2	−28.1	0
Southern margin	Kayindike	41	K11	J_3q	4251–4256	40.7	−26.6	0
Northwestern part	Chepaizi Uplift	42	P2	N_1s	1013	40.3	−26.3	0
		43	C95	N_1s	471.05	40.7	−26.6	0
		44	CF13	N_1s	684–689	37.3	−26.9	0
		45	CF15	N_1s	584–590	34.2	−26.9	0
		46	CF19	N_1s	772–777	37.0	−26.5	0

[a] PM rank: Biodegradation rank based on extent of destruction of compound class developed by Peters and Moldowan (1993).

2005; Shen and Li, 2008; Zhang et al., 2014; Chang et al., 2018). According to the sequence of the resistance to biodegradation among compound classes in crude oils (e.g., *n*-alkanes < isoprenoids < steranes < hopanes < diasteranes, etc.), a ten-point scale (PM rank 1 to 10) of biodegradation has been proposed by Peters and Moldowan (1993) and is widely used for assessing the extent of biodegradation, with PM rank 1 indicating a slight extent and PM rank 10 indicating an extreme extent of biodegradation.

In the present study, two suites of genetically related crude oils, each including both non-biodegraded (as reference oils) and slight to moderate biodegraded (PM rank 1 − 4) oils, were chosen for comparative study. According to the study of Jiang et al. (2019), the first suite of crude oils from the Mahu depression along the northwestern margin of the basin (Table 1; Nos. 1–10) has a relatively low maturity and a low concentration of diamondoids (mostly < 100 ppm). These oils are considered to be sourced from the middle Permian lower Wuerhe Formation (P_2w) in the Mahu Depression (Chen et al., 2016a, b; Huang, 2017). The second suite of crude oils from the Shinan and Luliang oilfields in the central basin (Table 1; Nos. 21–30) have entered the mature stage and contain > 200 ppm diamondoids. These oils are considered to have been generated from the relatively higher mature P_2w source rocks in the Pen 1 Jingxi Depression (Pan et al., 1999, 2003; Wang et al., 2001; Zou et al., 2005; Chen et al., 2010; Jiang et al., 2019).

The biodegradation levels of the two suites of crude oils were evaluated according to the PM scale (Peters and Moldowan, 1993) (Table 1). Most of these oils are lightly biodegraded (PM rank 1 − 3; e.g., *n*-alkanes are slightly, moderately, and severely biodegraded, respectively). Some oils (HW8, L27-1, and L103) have experienced moderate degradation (PM rank ≥ 3) and only contain trace amounts of *n*-alkanes. As the selective removal of crude oil compounds by biodegradation, *n*-alkanes are clearly affected in the slight to moderate biodegradation stages (PM rank 1 − 4), whereas the isoprenoids, such as pristane and phytane, are unaffected (Peters and Moldowan, 1993). Present result shows the consistent trend as Pr/*n*-C_{17} and Ph/*n*-C_{18} increase with increasing biodegradation in the two suites of crude oils (Table 2). In addition, the API gravity values of these oils decrease with increasing biodegradation, particularly for the suite of crude oils from the central basin (Table 1). This can be attributed to the preferential depletion of light compounds in crude oils due to biodegradation.

Fig. 2 shows gas chromatograms and m/z 191 mass fragmentograms of typical biodegraded oils from the central part of the Junggar Basin

Table 2
Geochemical parameters for crude oil samples from the Junggar Basin.

No.	Sample name	As (ppm)	Ds (ppm)	Dias (ppm)	Pr/Ph	Pr/n-C_{17}	Ph/n-C_{18}	C_{29}ααα20S/(20S + 20R)	C_{29}αββ/(ααα + αββ)	T/(T + P)	MAI
1	X89	97.0	2.6	99.6	1.02	1.02	1.14	0.46	0.58	0.80	0.52
2	W42	40.4	1.3	41.7	0.90	1.15	1.34	0.44	0.44	0.61	0.54
3	H94	83.8	2.0	85.9	1.04	0.80	0.86	0.42	0.45	0.50	0.53
4	X71	38.0	1.0	39.1	0.78	1.05	1.44	0.46	0.59	0.49	0.43
5	X7202	44.9	1.5	46.4	1.01	1.05	1.19	0.47	0.58	0.79	0.39
6	HS4	167.3	8.7	176.0	1.11	1.15	0.99	0.45	0.54	0.66	0.56
7	W007	48.9	1.0	50.0	0.88	1.52	2.08	0.44	0.51	0.6	0.52
8	HW5	67.7	1.8	69.6	1.09	1.18	1.24	0.47	0.59	0.71	0.49
9	K129	105.1	3.4	108.4	0.85	1.23	1.63	0.46	0.54	0.67	0.44
10	HW8	77.3	2.1	79.4	0.65	1.52	2.78	0.46	0.56	0.69	0.52
11	MA134	252.1	13.6	265.7	1.21	0.86	0.78	0.47	0.61	0.81	0.50
12	MA15	419.8	44.0	463.8	1.34	0.90	0.74	0.48	0.63	0.86	0.51
13	MA18	212.7	5.8	218.4	1.15	0.92	0.84	0.48	0.70	0.83	0.54
14	MX1	187.3	5.2	192.5	1.11	0.85	0.81	0.48	0.67	0.83	0.54
15	DA9	219.4	7.9	227.3	1.16	0.74	0.65	0.46	0.70	0.84	0.53
16	DT1	300.6	18.8	319.4	1.13	0.96	0.94	0.47	0.62	0.94	0.55
17	XG1	411.5	20.3	431.9	1.20	0.57	0.54	0.49	0.64	0.93	0.52
18	K901	238.4	15.5	253.9	1.44	0.44	0.32	0.46	0.60	0.50	0.49
19	G25	265.5	14.1	279.6	1.91	0.33	0.18	0.48	0.60	0.54	0.43
20	HS6	290.4	15.3	305.7	1.21	0.61	0.54	0.45	0.55	0.73	0.49
21	SN60	230.3	13.8	244.1	1.51	0.39	0.27	0.46	0.59	0.52	0.47
22	SN62	222.6	15.5	238.1	1.52	0.33	0.24	0.48	0.59	0.52	0.47
23	L11	325.0	16.2	341.2	1.37	0.37	0.29	0.46	0.60	0.61	0.45
24	L12	282.7	11.1	293.8	1.48	0.34	0.23	0.46	0.59	0.46	0.47
25	L27-2	346.2	22.8	369.0	1.56	0.41	0.28	0.45	0.60	0.58	0.45
26	SN42	390.5	20.3	410.9	1.59	0.80	0.47	0.48	0.59	0.56	0.43
27	L9-1	789.1	49.8	838.8	1.35	2.75	1.30	0.46	0.60	0.59	0.52
28	L9-2	415.4	28.4	443.7	1.44	7.93	2.53	0.47	0.59	0.60	0.45
29	L27-1	406.1	33.4	439.5	1.51	6.38	6.69	0.47	0.60	0.58	0.46
30	L103	935.0	64.0	999.1	0.56	8.10	22.50	0.46	0.60	0.61	0.51
31	DX21-1	344.2	11.0	355.2	2.70	0.18	0.07	0.41	0.53	0.22	0.43
32	DX21-2	347.6	17.3	364.9	2.15	0.17	0.08	0.37	0.56	0.18	0.43
33	DX10-1	587.4	9.8	597.2	3.11	0.29	0.18	0.25	0.45	0.16	0.56
34	DX10-2	1578.7	149.7	1728.4	2.20	0.19	0.11	0.26	0.46	0.19	0.61
35	DX14-1	498.1	17.3	515.4	3.00	0.37	0.16	0.32	0.46	0.22	0.53
36	DX14-2	606.1	41.7	647.8	1.54	0.22	0.17	0.41	0.58	0.68	0.52
37	D403-1	541.1	32.2	573.3	1.36	0.18	0.16	0.34	0.57	0.78	0.50
38	D403-2	1284.3	136.1	1420.4	1.60	0.21	0.16	0.35	0.58	0.66	0.51
39	DX17-1	614.4	28.9	643.2	1.35	0.15	0.13	0.45	0.62	0.75	0.51
40	DX17-2	1066.0	29.8	1095.8	1.45	0.19	0.14	0.39	0.55	0.63	0.57
41	K11	584.7	56.7	641.4	3.23	0.25	0.08	0.48	0.59	0.12	0.34
42	P2	446.3	44.5	490.8	2.28	0.30	0.13	0.36	0.48	0.13	0.37
43	C95	513.7	39.4	553.1	2.29	0.26	0.12	0.36	0.48	0.13	0.38
44	CF13	548.0	48.3	596.3	2.15	0.26	0.12	0.36	0.47	0.12	0.38
45	CF15	684.4	68.0	752.4	2.29	0.38	0.17	0.36	0.48	0.12	0.38
46	CF19	1183.9	89.6	1273.5	1.82	0.22	0.12	0.35	0.49	0.13	0.30

(*continued on next page*)

Table 2 (*continued*)

No.	EAI	DMAI-1	DMAI-2	TMAI-1	TMAI-2	MAs/A	DMAs/A	DMAs/MAs	MDs/D	DMDs/D	DMDs/MDs
1	0.27	0.47	0.32	0.24	0.31	4.27	11.77	2.76	–	–	0.80
2	0.32	0.51	0.37	0.27	0.33	3.44	8.00	2.33	–	–	–
3	0.27	0.51	0.36	0.25	0.32	3.39	7.15	2.11	–	–	0.95
4	0.28	0.40	0.30	0.17	0.25	3.17	6.95	2.19	–	–	–
5	0.25	0.35	0.26	0.15	0.24	6.14	22.17	3.61	–	–	0.84
6	0.26	0.51	0.36	0.24	0.32	3.94	9.26	2.35	1.76	1.48	0.84
7	0.30	0.48	0.35	0.25	0.32	3.73	8.77	2.35	–	–	–
8	0.25	0.55	0.38	0.32	0.36	3.83	5.58	1.46	–	–	–
9	0.26	0.52	0.34	0.26	0.33	4.53	7.80	1.72	–	–	–
10	0.32	0.54	0.36	0.28	0.34	4.06	6.41	1.58	–	–	–
11	0.28	0.49	0.33	0.23	0.31	5.04	13.13	2.60	3.04	4.07	1.34
12	0.28	0.51	0.30	0.17	0.24	8.83	21.50	2.43	4.48	5.62	1.25
13	0.23	0.48	0.31	0.22	0.28	5.19	14.43	2.78	–	–	1.08
14	0.24	0.49	0.32	0.24	0.29	5.04	13.61	2.70	–	–	1.31
15	0.22	0.47	0.30	0.22	0.29	5.05	14.56	2.88	–	–	1.43
16	0.22	0.59	0.38	0.21	0.27	7.25	15.69	2.16	–	–	1.43
17	0.28	0.54	0.36	0.39	0.43	2.63	6.36	2.41	3.55	2.90	0.82
18	0.23	0.50	0.35	0.25	0.32	3.76	8.73	2.32	1.55	1.27	0.82
19	0.18	0.47	0.31	0.23	0.30	2.85	6.08	2.13	0.94	0.33	0.35
20	0.28	0.50	0.34	0.28	0.36	3.98	9.80	2.46	3.10	3.36	1.08
21	0.22	0.51	0.35	0.27	0.35	3.40	7.39	2.17	1.55	1.35	0.87
22	0.23	0.50	0.36	0.27	0.34	3.34	7.15	2.14	1.74	1.32	0.76
23	0.20	0.50	0.33	0.32	0.39	2.56	5.68	2.22	2.09	1.41	0.67
24	0.22	0.50	0.34	0.31	0.38	3.05	6.84	2.24	1.69	1.42	0.84
25	0.23	0.51	0.34	0.36	0.41	2.33	5.04	2.17	1.76	1.16	0.66
26	0.24	0.50	0.33	0.39	0.42	2.43	4.85	2.00	1.81	0.92	0.51
27	0.22	0.50	0.33	0.26	0.34	3.71	7.47	2.01	1.82	1.03	0.57
28	0.28	0.51	0.34	0.37	0.41	2.49	5.23	2.10	1.91	1.30	0.68
29	0.27	0.51	0.35	0.38	0.42	2.42	5.19	2.14	1.78	1.35	0.76
30	0.24	0.49	0.32	0.25	0.33	3.75	7.98	2.13	1.73	1.08	0.63
31	0.20	0.51	0.33	0.24	0.36	2.45	5.01	2.04	2.06	0.53	0.26
32	0.22	0.50	0.33	0.23	0.36	2.30	4.70	2.04	1.45	0.41	0.28
33	0.31	0.63	0.42	0.33	0.46	2.58	5.41	2.10	1.40	0.70	0.50
34	0.43	0.67	0.48	0.33	0.47	3.65	7.79	2.14	4.44	2.57	0.58
35	0.30	0.60	0.40	0.32	0.46	2.47	4.91	1.98	0.77	0.46	0.60
36	0.36	0.58	0.40	0.30	0.45	2.64	5.02	1.90	2.51	1.32	0.52
37	0.33	0.56	0.38	0.29	0.44	2.68	5.21	1.94	2.28	1.17	0.51
38	0.28	0.61	0.43	0.24	0.38	6.97	14.46	2.08	1.64	0.69	0.42
39	0.35	0.58	0.39	0.28	0.42	2.98	6.41	2.15	4.84	3.03	0.63
40	0.27	0.70	0.48	0.31	0.43	5.49	10.01	1.82	4.57	2.25	0.49
41	0.17	0.43	0.25	0.16	0.25	4.63	7.43	1.61	1.96	0.49	0.25
42	0.27	0.45	0.28	0.23	0.35	2.74	5.61	2.05	1.36	0.47	0.34
43	0.29	0.46	0.29	0.25	0.38	2.83	4.99	1.76	1.41	0.44	0.31
44	0.31	0.46	0.28	0.25	0.37	2.93	5.28	1.80	1.48	0.49	0.33
45	0.30	0.47	0.28	0.25	0.36	3.09	5.42	1.76	1.00	0.36	0.36
46	0.19	0.49	0.28	0.16	0.22	5.16	9.47	1.83	1.07	0.32	0.30

Note: As: adamantanes; Ds: diamantanes; Dias: diamondoids; Pr/Ph: pristane/phytane; Pr/n-C_{17}: pristane/normal heptadecane; Ph/n-C18: phytane/normal octadecane; C_{29}ααα20S/(20S + 20R): C_{29} ααα-stigmastane 20S/(20S + 20R); C29αββ/(ααα+αββ): C_{29} stigmastane αββ/(ααα+αββ); T/(T + P): tricyclic/(tricyclic + pentacyclic) terpane; MAI: 1-MA/(1-MA + 2-MA); EAI: 1-EA/(1-EA + 2-EA); DMAI-1: 1,3-DMA/(1,3-DMA + 1,2-DMA); DMAI-2: 1,3-DMA/(1,3-DMA + 1,4-DMA); TMAI-1: 1,3,5-TMA/(1,3,5-TMA + 1,3,4-TMA); TMAI-2: 1,3,5-TMA/(1,3,5-TMA + 1,3,6-TMA); MAs/A: Methyladamantanes/Adamantane; DMAs/A: Dimethyladamantanes/Adamantane; DMAs/MAs: Dimethyladamantanes/Methyladamantanes; MDs/D: Methyldiamantanes/Diamantane; DMDs/D: Dimethyldiamantanes/Diamantane; DMDs/MDs: Dimethyldiamantanes/Methyldiamantanes; symbol "-": no detection.

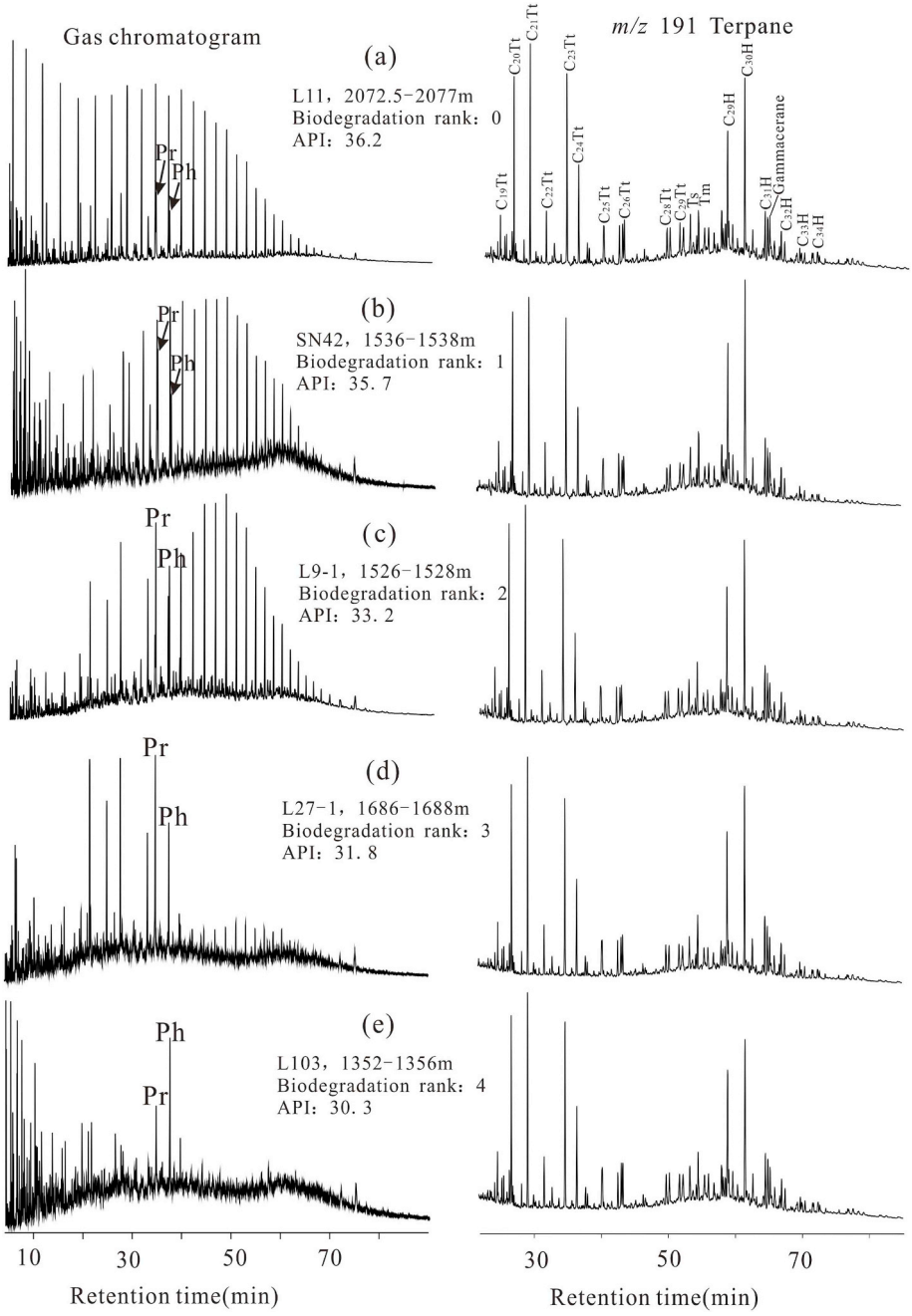

Fig. 2. Gas chromatograms and m/z 191 mass fragmentograms of typical biodegraded oils from the central Junggar Basin, showing PM ranks of 0–4 with increasing degradation on *n*-alkanes but no alteration on terpanes.

with PM ranks of 0–4. The L11 oil represents a non-biodegraded oil. The L103 oil is the most severely biodegraded sample among the studied oils. Its biodegradation level reaches PM rank 4, given that all of the *n*-alkanes have been degraded, the isoprenoids are partially degraded, and the terpanes are completely intact which has a same distribution as the PM rank 0 sample. And the same distribution of terpanes in the five samples in Fig. 2 suggests biodegradation has little effect on the terpanes at PM ranks of 0–4. Moreover, the PM rank increases as the reservoir depth decreases (Fig. 2; Table 1), which is consistent with the occurrence of more significant microbial activity in shallower strata.

A change in oil diamondoid concentrations might occur at a relatively low biodegradation level. The concentration of total diamondoids (e.g., sum of adamantanes and diamantanes) tends to increase with increasing biodegradation level from PM rank 0 to 4 for the oils from the central basin, but does not change noticeably for oils from the northwestern basin (Fig. 3a). With decreasing API gravity values, diamondoid concentrations increase in oils from the central basin, but change little in oils from the northwestern basin (Fig. 3b). It seems that elevated diamondoids concentration depends to a large extent on the initial diamondoids concentration of the original hydrocarbon. As stated earlier, oils from the northwestern basin have a relatively low maturity and a low diamondoid concentration, and the increase of diamondoid concentrations caused by slight to moderate biodegradation on these oils seems to be non-obvious, which might attribute to the disability to reliably detection of diamomdoid composition in a very low concentration. While, for the mature oils from the central basin which have abundant diamondoids, biodegradation appears to have caused more significant variations in diamondoid concentrations. Previous studies have suggested that diamondoids are not affected by slight

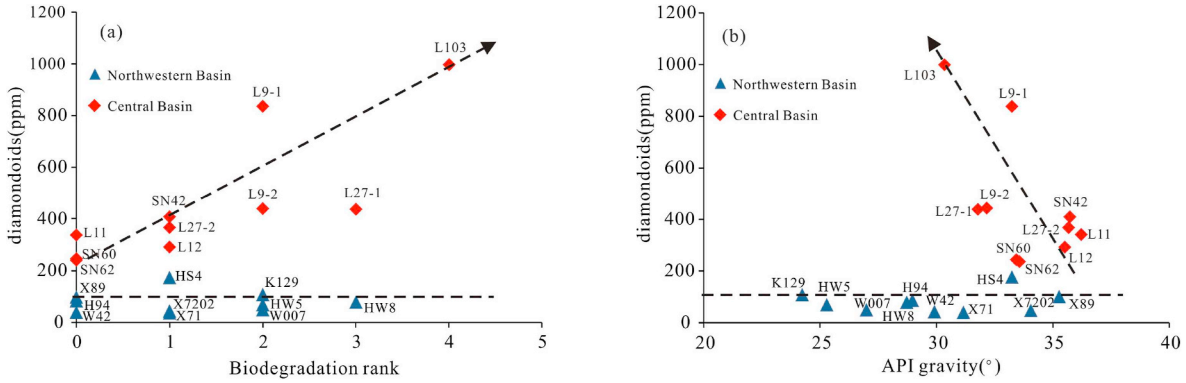

Fig. 3. (a) Concentration of total diamondoids vs. biodegradation rank and (b) concentration of total diamondoids vs. API gravity values for biodegraded oils from the Junggar Basin, showing biodegradation results in obviously increasing of total diamondoid concentrations for oil samples from the central basin but no significant changes for oil samples from the northwestern basin.

biodegradation (Grice et al., 2000; Wei et al., 2007), and the biodegradation resistance of diamondoids is similar to that of terpanes (Wei et al., 2007). As such, the loss of readily biodegraded components (e.g., *n*-alkanes, *i*-alkanes, and isoprenoids) in oils could account for the increasing concentrations of total diamondoids in slightly to moderately biodegraded oils (PM ranks 1 − 4). Theoretically, during biodegradation the abundance of diamondoids could keep increasing until the onset of diamondoid biodegradation. Hence, for the oils that underwent moderate biodegradation, when *n*-alkanes and isoprenoids were completely degraded and terpanes began to be biodegraded, the concentration of total diamondoids might reach a maximum. Given that normal and branched paraffins typically constitute about 35% − 50% of a non-biodegraded oil, their removal can increase the diamondoid concentration by a factor of 1.3–2.0. The diamondoid concentration of the L103 oil (PM rank 4) might be double that of non-biodegraded oil (L11) from the same oilfield (Table 2), which is consistent with the above inference.

Variations in diamondoid concentration ratios and isomerization ratios can indicate different biodegradation levels, given that the resistance to biodegradation varies among the diamondoid compounds. For example, adamantanes are more susceptible to biodegradation than diamantanes and triamantanes, and adamantanes might be altered at a PM rank of 3, and the methyl adamantanes/adamantane ratio (MAs/A) would increase with increasing biodegradation, with significant changes occurring at a PM rank of 5 (Wei et al., 2007). In present study, take the suite of oils from the central basin for an instance, at relatively low biodegradation levels, MAs/A and dimethyl adamantanes/adamantane (DMAs/A) ratios for the studied oils do not show significant differences with increasing biodegradation, with MAs/A ranging from 2.33 to 3.75 (most in 2.33–3.40) and DMAs/A varying in the range of 4.85–7.98 (most in 5.68–7.39) (Table 2). And there are no obvious variations in methyl diamantanes/diamantane (MDs/D) and dimethyl diamantanes/diamantane (DMDs/D) ratios, with MDs/D and DMDs/D distributing in the ranges of 1.55–2.09 (most in 1.69–1.91) and 0.92–1.42 (most in 1.30–1.42), respectively (Table 2). The results are consistent with the study of Wei et al. (2007). Grice et al. (2000) suggested that diamantanes might be affected by severe levels of biodegradation, which would be responsible for the limited variation of these ratios (e.g., MDs/D and DMDs/D).

Variations in diamondoid isomerization ratios (e.g., MAI, EAI, DMAI-1, DMAI-2, TMAI-1, and TMAI-2) are not obvious for the same suite of oils at PM ranks of 0–4 (Table 2). For example, the suite of biodegraded and non-biodegraded oils from the central basin has almost constant DMAI-1 0.49–0.51, average 0.50) and DMAI-2 (0.32–0.36, average 0.34) values. This suggests that the effect of slight to moderate biodegradation on diamondoid isomerization ratios is negligible, which is consistent with the results of previous studies (Grice et al., 2000; Wei et al., 2007; Cheng et al., 2018). In fact, even severe biodegradation (PM rank 8) only has a slight effect on diamondoid isomerization ratios, apart from EAI (Cheng et al., 2018). This might be attributed to the diamondoid isomers having little variability in their susceptibility to biodegradation (e.g., 1-MA vs. 2-MA and 1,3-DMA vs. 1,2-DMA). Therefore, diamondoid isomerization ratios can still be used as maturity indicators in severely biodegraded oils.

Slight to moderate biodegradation can result in an increase of diamondoid concentrations in mature oils with relatively abundant diamondoids. In contrast, the concentration ratios (e.g., MAs/A, DMAs/A, MDs/D, and DMDs/D) and isomerization ratios are not significantly affected by moderate biodegradation. Variations in these parameters can be used to identify severely biodegraded oils.

3.2. Water washing

Light oils from the Neogene Shawan Formation (N_1s) in the Chepaizi Uplift, northwestern Junggar Basin, are characterized by very shallow burial depths (< 1000 m), low densities (API > 34°), and relatively heavy carbon isotopes (greater than −27‰) (Table 1). Oil–source correlations suggest that the N_1s light oils in the Chepaizi area are mixed, derived mainly from high-mature Jurassic coal measures and dissolved, relatively low-maturity biomarker-rich Cretaceous bitumen (Zhang et al., 2010b; Liu et al., 2011; Xiao et al., 2014). The K11 light oil was only derived from the Jurassic coal measures and has experienced no obvious reservoir alteration according to its gas chromatogram in Fig. 4. Therefore, it represents an end-member oil composition from the Jurassic coal measures. Sterane-based maturity ratios, such as C_{29}ααα 20S/(20S + 20R) and C_{29}αββ/(ααα+αββ) in the K11 light oil are obviously higher (0.48 and 0.59, respectively) than those in the N_1s light oils (0.35–0.36 and 0.47–0.49, respectively), indicating that the K11 light oil has a significantly higher maturity than the N_1s light oils (Table 2). According to previous studies, it can be attributed to the mixing of low-maturity oils into the N_1s light oils (Zhang et al., 2010b; Liu et al., 2011; Xiao et al., 2014).

However, the maturity indicated by the diamondoid concentrations of the N_1s light oils and end-member K11 oil are inconsistent with their biomarker-based maturities. In general, the higher-maturity oils should contain more abundant diamondoids (Jiang et al., 2019), and thus it is inferred (from biomarker-based maturity indices) that the diamondoid concentrations in the N_1s light oils should be much less than that of the higher-maturity K11 oil. However, diamondoid concentrations in most N_1s light oils are close to that in the K11 oil, and some oils (e.g., CF15 and CF19) even have higher diamondoid concentrations than the K11 oil (Table 2). Additionally, the similar stable carbon isotopic compositions of the N_1s light oils indicate similar mixing proportions of each end-member oils, which thus cannot explain the substantial variations of diamondoid concentrations among the N_1s light oils. Thus, we

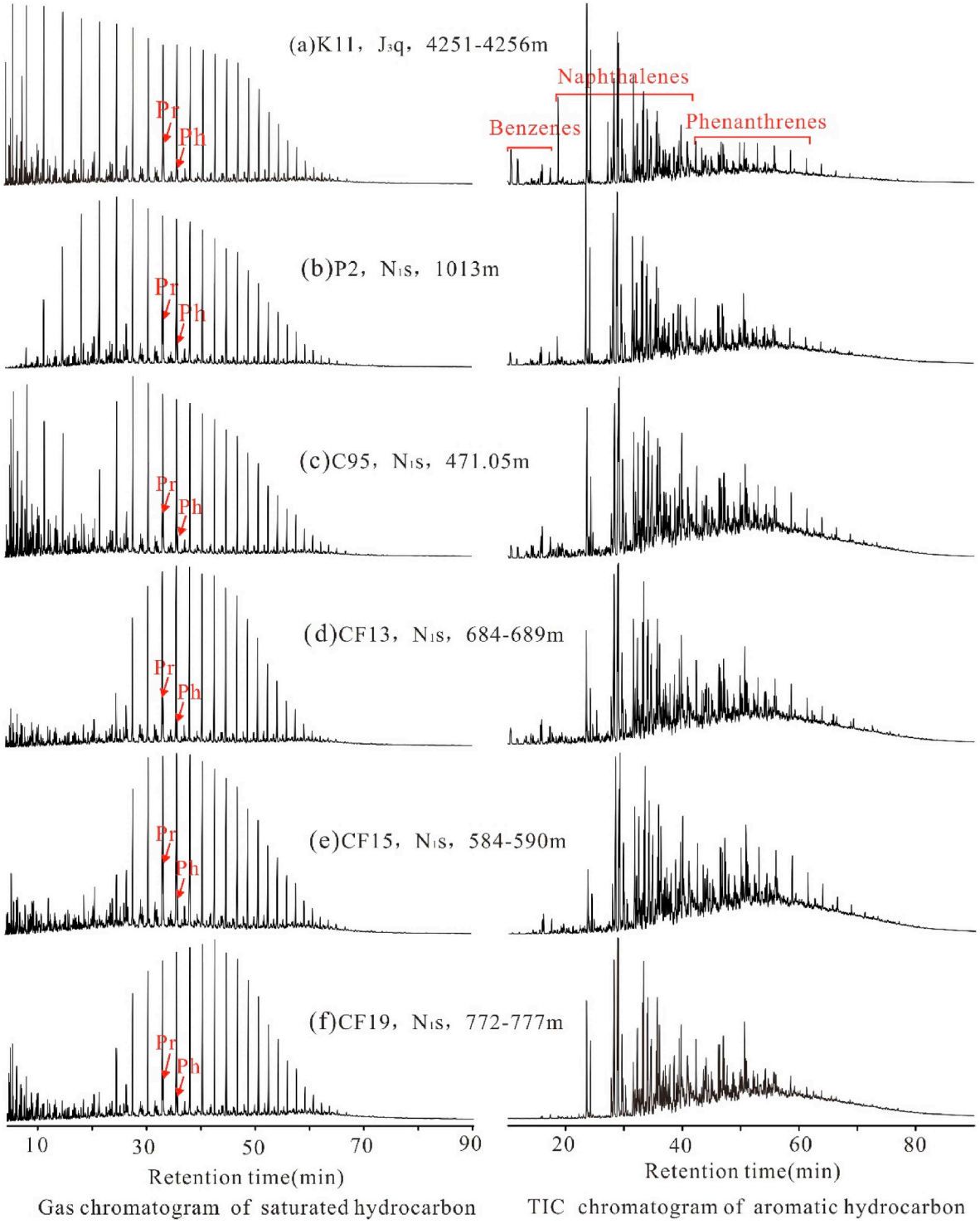

Fig. 4. Gas chromatograms of saturated hydrocarbons and TIC chromatograms of aromatic hydrocarbons for light oils from the Chepaizi Uplift, northwestern Junggar Basin, showing different degrees of water washing on the C_{15-} fractions.

propose that some reservoir alteration affected these N_1s light oils and led to the variations in diamondoid concentrations. The C_{15-} fractions (including saturated and aromatic fractions) of these N_1s light oils, particularly for CF13, CF15, and CF19, are partially or mostly removed, whereas the end-member K11 oil contains a relatively complete inventory of these fractions (Fig. 4). In contrast, the C_{15+} saturated fractions in these light oils do not appear to have experienced obvious alteration. As such, biodegradation can be excluded, as it selectively removes hydrocarbons in the following sequence: *n*-alkanes, isoprenoids, steranes and hopanes, and aromatics (Peters et al., 2005). Also, the typical UCM (unresolved complex mixtures) hump resulted from biodegradation has not been observed in these N_1s light oils. We suggest that water washing might be mainly responsible for the compositional alteration of these N_1s light oils, as water washing is particularly effective in the removal of the C_{15-} fractions and hydrocarbons are removed in the order of aromatics > *n*-alkanes > naphthenes (Lafargue and Barker, 1988; Sarmah and Raju, 2016), which is consistent with the compositional variations depicted in Fig. 4. The

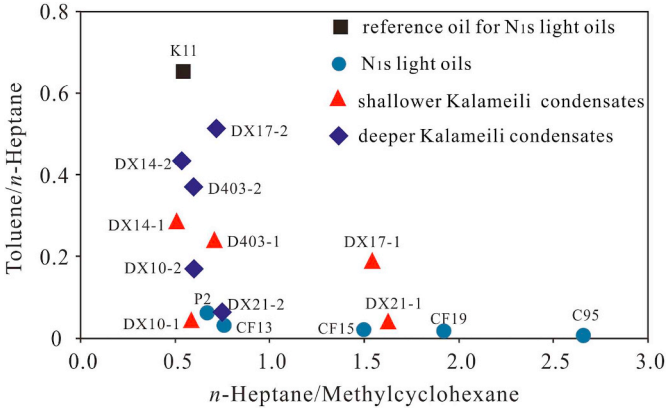

Fig. 5. Plot of toluene/*n*-heptane vs. *n*-heptane/methylcyclohexane for N_1s light oils and Kalameili condensates. The very low aromaticity ratios (toluene/*n*-heptane) of the N_1s light oils reflecting the water washing effect on these oils, and the lower aromaticity ratios and higher paraffinity ratios (*n*-heptane/methylcyclohexane) of the shallower Kalameili condensates relative to the deeper ones in a same well suggesting the shallower oils might be formed by gas washing.

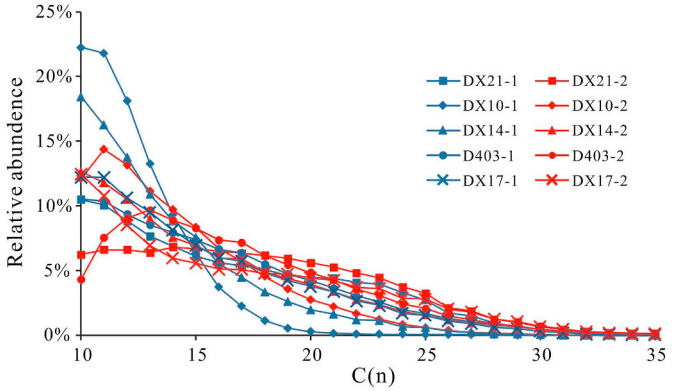

Fig. 6. Relative abundances of *n*-alkanes in oils from the Kalameili gas field, eastern Junggar Basin, showing more abundance of *n*-C_{15-} hydrocarbons in the shallower samples (blue symbol) relative to the deeper ones (red symbol). (For interpretation of the references to colour in this figure legend, the reader is referred to the Web version of this article.)

diagram of aromaticity ratio (toluene/*n*-heptane) versus paraffinity ratio (*n*-heptane/methylcyclohexane) shows that the N_1s light oils have very low aromaticity ratio (< 0.1), which are far less than that of the K11 oil (Fig. 5). It suggests that water washing has occurred and the low molecular weight aromatic compounds in the N_1s light oils are extracted by water (Thompson, 1987). The diamondoids are a type of naphthenes with relatively high molecular weight, which are difficult to remove by water washing comparing to low molecular weight aromatics and *n*-alkanes. Hence, water washing could increase the diamondoid concentration in oils, depending on the degree of water washing. If other alteration effects are excluded, then more severe water washing leads to a greater increase in diamondoid concentration. The diamondoid concentrations increase from the P2 (490.8 ppm), C95 (553.1 ppm), CF13 (596.3 ppm), CF15 (752.4 ppm), to CF19 (1273.5 ppm) oils (Table 2), reflecting progressively greater water washing of these N_1s light oils. Both low molecular weight aromatic hydrocarbons (e.g., benzenes and some naphthalenes) and C_{15-} saturated hydrocarbons are absent in the CF19 oil, also suggesting it has suffered from the most severe water washing (Fig. 4).

In contrast, water washing has no obvious effects on diamondoid isomerization and concentration ratios. The diamondoid isomerization ratios in these N_1s light oils are almost identical (e.g., 0.37–0.38, 0.27–0.31, 0.23–0.25, and 0.35–0.38 for MAI, EAI, TMAI-1, and TMAI-2, respectively), except for the CF19 oil (e.g., 0.30, 0.19, 0.16, and 0.22 for MAI, EAI, TMAI-1, and TMAI-2, respectively) (Table 2) that has experienced the most severe water washing. This indicates that isomerization ratios of diamondoids are insensitive to water washing, unless it has been severe. Similarly, no significant changes in diamondoid concentration ratios (e.g., mainly in 2.74–3.09, 4.99–5.61, 1.76–2.05, 1.00–1.48, 0.32–0.49 and 0.30–0.36 for MAs/A, DMAs/A, DMAs/MAs, MDs/D, DMDs/D, and DMDs/MDs, respectively) among these N_1s light oils are observed, except for MAs/A and DMAs/A ratios in the CF19 oil (5.16 and 9.47 for MAs/A and DMAs/A, respectively) (Table 2). This might be due to the partial remove of adamantane (A) in the CF19 oil by severe water washing. This suggests that most diamondoid concentration ratios are stable even after severe water washing, apart from some indices involving adamantane (e.g., MAs/A and DMAs/A).

In summary, the discrepancy between the biomarker maturity indices and diamondoid concentrations in the oils might have resulted from water washing, which invalidates the use of diamondoid concentrations as an index of oil maturity. However, water washing has insignificant effects on diamondoid isomerization and concentration ratios unless severe water washing has occurred.

3.3. Gas washing

The Kelameili gas field, located in the eastern Junggar Basin, is the largest gas field in the basin and produces condensates associated with natural gas. Although previous studies have suggested that oil and gas in the Kelameili gas field were generated from highly mature Carboniferous type III kerogen (Da et al., 2010; Yang et al., 2012; Long et al., 2014; Yu et al., 2014; Xiang et al., 2016), some interesting phenomenon has been found in some samples in present study, which may reflect different formations of the condensates. Here, five pairs of oils (DX21-1–DX21-2; DX10-1–DX10-2; DX14-1–DX14-2; D403-1–D403-2; DX17-1–DX17-2), each from the same well but at different depths, were collected from the Kelameili gas field (Table 1) to investigate the formation of condensates in this field.

The oils from different depths in each well have different API gravities and stable carbon isotopic compositions (Table 1). Generally, the shallower oils have higher API gravities and slightly heavier $\delta^{13}C$ values than the deeper oils in each well. Fig. 6 shows that the shallower oils are enriched in *n*-C_{15-} hydrocarbons, but depleted in *n*-C_{15+} hydrocarbons, relative to the deeper oils. The above differences of hydrocarbon composition and physicochemical properties between the shallower and deeper condensates indicate that the shallower condensates have a higher maturity than the deeper ones in a same well. Previous studies have reported multiple stages of hydrocarbon generation and charging in the Kelameili gas field. The condensates were generated from highly mature Carboniferous source rocks and charged the deeper reservoirs at an early stage, and natural gas was generated from more highly mature Carboniferous source rocks and recharged the reservoirs (including the former charged and uncharged reservoirs) at a later stage (Da et al., 2010; Yang et al., 2012). Thus, hydrocarbon charges in different maturity stages could be used to explain the different maturites of the oils from different depths in the same well. In general, a higher thermal maturity leads to more abundant diamondoids in oils (Jiang et al., 2019). However, the total diamondoids are less abundant in the shallower oils than in the deeper oils in each well, particularly for oils from the DX10 (597 ppm and 1728.4 ppm for the shallower and deeper ones, respectively), D403 (573.7 ppm and 1420.4 ppm for the shallower and deeper ones, respectively), and DX17 (643.2 ppm and 1095.8 ppm for the shallower and deeper ones, respectively) wells (Table 2). In addition, if the condensates were all originated from the highly mature source rocks concluded in previous

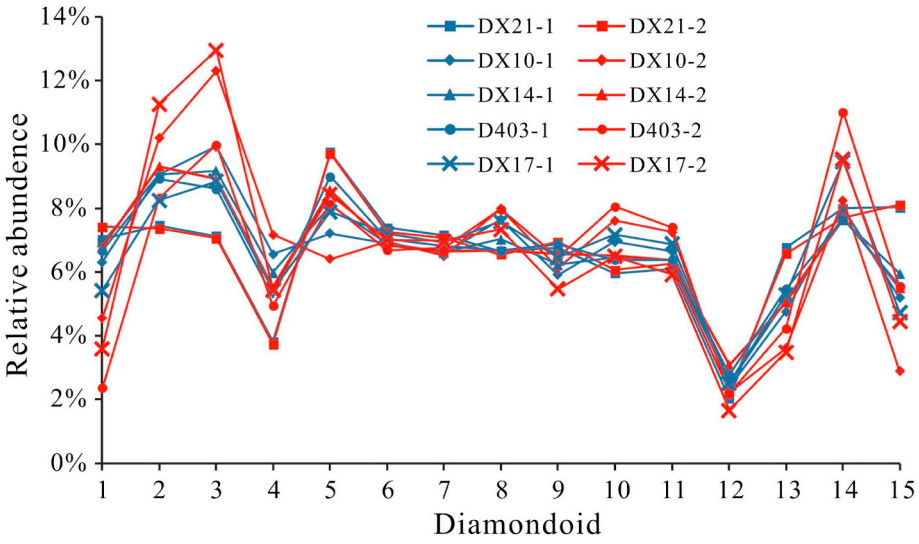

Fig. 7. Relative abundances of diamondoids in oils from Kelameili gas field, eastern Junggar Basin, showing gas washing causes the increasing of relative contents of 1-MA and 1,3-DMA in the deeper oil samples (red symbol) comparing to the shallower ones (blue symbol). 1: A; 2: 1-MA; 3: 1,3-DMA; 4: 1,3,5-TMA; 5: 2-MA; 6: 1,4-DMA(cis); 7: 1,4-DMA(trans); 8: 1,3,6-TMA; 9: 1,2-DMA; 10: 1,3,4-TMA(cis); 11: 1,3,4-TMA(trans); 12: 1-EA; 13: 2,6 + 2,4-DMA; 14: 1,2,3-TMA; 15: 2-EA. (For interpretation of the references to colour in this figure legend, the reader is referred to the Web version of this article.)

studies (Da et al., 2010; Yang et al., 2012), such condensates should typically contain a higher concentration of diamondoids (> 1000 ppm) (Jiang et al., 2019). However, diamondoid concentrations in most of these condensates are much lower than 1000 ppm, especially for the shallower condensates (e.g., 355.2 ppm, 597.2 ppm, 515.4 ppm, 573.3 ppm, and 643.2 ppm for DX21-1, DX10-1, DX14-1, D403-1, and DX17-1, respectively) (Table 2). As such, condensates studied here should not be formed by thermal cracking in the high mature stage, and the physicochemical differences of oils from different depth in each well might not be due to hydrocarbon charges in different maturity stages. Condensates can also be generated from evaporative/phase-controlled molecular fractionation of normal oils caused by gas washing (Thompson, 1987, 1988; 2010, 2016; Larter and Mills, 1991; Zhang, 2000). As stated earlier, natural gas recharge has ever happened in the Kelameili gas field (Da et al., 2010; Yang et al., 2012), thus, we propose that condensates here might be resulted from phase fractionation caused by gas washing.

Gas washing of oil is a common reservoir alteration process (Curiale and Bromley, 1996; Meulbroek et al., 1998; Losh et al., 2002; Cui et al., 2012; Chen et al., 2015). It is caused mainly by the intrusion of natural gas into an early formed oil reservoir, whereby large amounts of gas can preferentially dissolve low-molecular-weight *n*-alkanes from the oils into a coexisting vapor phase. The vapor phase then migrates upward and is trapped in a shallower reservoir. With decreasing temperature and pressure, the trapped vapor condenses, experiences hydrocarbon phase fractionation, and forms a gas phase (natural gas) and liquid phase (gas condensate). The procedure is related to the depth of the reservoir, i.e., the shallower the reservoir is, the severer phase fractionation happens, leading to the more light-end compounds (n-C_{15-}) enriched in the shallower layers, which is consistent with the distribution of *n*-alkanes in the studied oils here (Fig. 6). According to the study of Thompson (1987, 1988), during the gas washing process, the *n*-heptane and methylcyclohexane tend to more favorably partition into the gaseous phase, that would result in a loss of *n*-heptane and methylcyclohexane and an enrichment of aromatics in the residual oils. As shown in Fig. 5, the shallower oils have relative lower aromaticity ratio (toluene/*n*-heptane) and higher paraffinity ratio (*n*-heptane/methylcyclohexane) than the deeper ones from a same well, indicating the shallower oils might be gas condensates fractionated from their original "parent" oils (which might not be the deeper ones in this study) by gas washing. In contrast to the behavior of light-end compounds (n-C_{15-}), due to the lower solubility of diamondoids in natural gas than low-molecular-weight *n*-alkanes (Zhang et al., 2010a), the condensates separated from the vapor are poor in diamondoids relative to the original oils, and the fractionation will be more and more obvious as the vapor migrates from a deep depth to a shallow depth. Thus, condensates formed by gas washing have a lower diamondoid concentration than the original oils, and the shallower condensates are poor in diamondoids relative to the deeper ones in a same well. This is consistent with the phenomenon observed in present study, that the diamondoid concentrations in most of the condensates here are lower than the condensates formed by thermal cracking (diamondoids > 1000 ppm, Jiang et al., 2019) and the shallower condensates have less diamondoids than the deeper ones in the same well.

The diamondoid isomerization ratios (e.g., MAI, DMAI-1, and DMAI-2) in the deeper condensates (e.g., DX10-2, D403-2, and DX17-2) are higher than those of the shallow condensates (e.g., DX10-1, D403-1, and DX17-1). Other isomerization ratios (e.g., EAI, TMAI-1, and TMAI-2) are similar or show inconsistent variations between the shallow and deep condensates (Table 2). The relative 1-MA and 1,3-DMA contents in the deeper condensates are higher than those of the shallower condensates (Fig. 7), this may explain the differences in MAI, DMAI-1, and DMAI-2 between the shallower and deeper condensates in each well. Similarly, the diamondoid concentration ratios (MAs/A and DMAs/A) of the deeper condensates (e.g., DX10-2, DX14-2, D403-2, and DX17-2) are higher than those of the shallower condensates (e.g., DX10-1, DX14-1, D403-1, and DX17-1). The other diamondoid concentration ratios (e.g., DMAs/MAs, MDs/D, and DMDs/MDs) are similar at different depths or show inconsistent variations.

As the discussion above, phase fractionation caused by gas washing would alter both the absolute concentrations and relative contents of diamondoids in oils. Consequently, some diamondoid isomerization ratios (e.g., MAI, DMAI-1, and DMAI-2) and concentration ratios (e.g., MAs/A and DMAs/A) would change in condensates formed by different extents of gas washing. Diamondoid absolute concentration can be used to differentiate between gas washing and thermal-cracking origins for condensates, e.g., if the diamondoid concentration in a high-mature condensate is much higher than 1000 ppm, it must be formed by thermal cracking, otherwise, it might be formed by gas washing.

3.4. Mixing

Although the oils from the northwestern part of the Junggar Basin were generated mainly from Permian source rocks, their diamondoid concentrations are distinct, and vary from 0 to 500 ppm (Jiang et al., 2019). This has been attributed mainly to the maturity difference of the source rocks from which these oils were generated (Jiang et al., 2019). In the present study, 20 oil samples (Nos. 1-20; Table 1) were collected from the northwestern margin of the basin to investigate the relationship between diamondoid concentrations and thermal maturity levels.

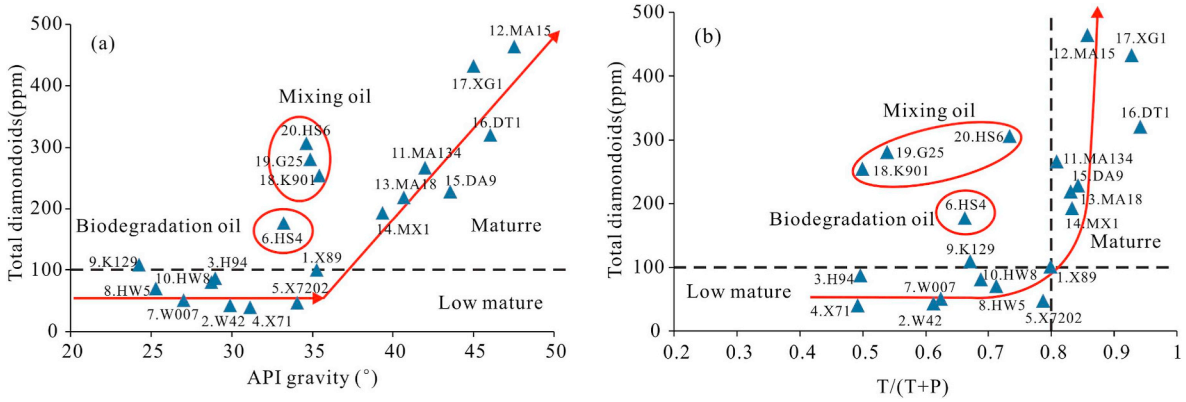

Fig. 8. (a) Total diamondoid concentrations vs. API gravity values and (b) total diamondoid concentrations vs. T/(T + P) values for oils from the northwestern Junggar Basin, showing mixing oil containing high diamondoid concentrations and low values of API gravity and T/(T + P).

According to diamondoid concentrations, API gravity values, and tricyclic/(tricyclic + pentacyclic) (T/(T + P)) ratios, 17 of these oils can be divided into two groups. One group is relatively low-mature oils (Nos. 1–10; Table 1), with a low content of diamondoids (mostly < 100 ppm), diamondoid concentrations that show no obvious variations with API gravity values, and low T/(T + P) values (Fig. 8). The diamondoid concentration in the HS4 oil (No. 6) is higher (> 100 ppm) than that in other oils in this low-mature oil group, which might be attributed to biodegradation mentioned in Section 3.1. The other group is relatively mature oils (Nos. 11–17; Table 1), which have relatively high contents of diamondoids (> 200 ppm), and high API gravity values (> 39°) and T/(T + P) values (> 0.8) (Fig. 8). Another maturity-related biomarker index also supports this classification, as C_{29} sterane αββ/(αββ+αα) values of the first group of oils are lower than those of the second group (Table 2). The biodegradation level of the first group of oils and its effects on the concentration of diamondoids was assessed in Section 3.1, which indicated that light biodegradation has no obvious effect on diamondoid concentration and thus will not seriously affect the maturity classification. No obvious biodegradation is observed in the second group of oils, and the variation in their diamondoid concentrations can be attributed to thermal maturity.

However, some oils, such as the K901, G25, and HS6 oils, yield contradictory thermal maturities from different methods. They are low-mature according to their low C_{29} sterane ββ/(ββ+αα) (0.67–0.71 = equilibrium) and T/(T + P) values, but mature according to their higher diamondoid concentrations (> 200 ppm). These anomalous oils (K901, G25, and HS6) have low API gravities and high diamondoid concentrations (Fig. 8a), which are inconsistent with the evolutionary trends exhibited by the two aforementioned groups of oils. Mixing could be a cause for this discrepancy, such as mixing between low-mature oils rich in biomarkers and mature oils rich in diamondoids. Previous studies have demonstrated that the petroleum system along the northwestern margin of the Junggar Basin is a hybrid system involving three sequences of source rocks with different maturities (e.g., the lower Permian Jiamuhe and Fengcheng formations and middle Permian lower Wuerhe Formation; Cao et al., 2005, 2006; Chen et al., 2016a, b; Liu et al., 2016). Hence, we suggest that these oils are mixtures derived from deeply buried and high-mature Permian source rocks and relatively low-maturity Permian source rocks.

There is no significant difference in diamondoid isomerization and concentration ratios between these mixed oils and the two aforementioned groups of oils (Table 2); and end members of the mixed oils cannot be constrained, so no further discussion is made on mixed oils in present study.

4. Conclusions

Diamondoid indices were used to investigate reservoir alteration (e.g., biodegradation, water washing, gas washing, and mixing) of oils collected from different areas of the Junggar Basin. The results indicate that slight to moderate biodegradation mainly affects the absolute diamondoid concentrations in the oils, rather than diamondoid concentration and isomerization ratios. This effect is more obvious for mature than low-mature oils, and can result in a factor of 1.3–2.0 increase in diamondoid concentrations for biodegraded mature oils as compared with non-biodegraded oils. As such, diamondoid concentration and isomerization ratios can be used to evaluate oil maturity even after light to moderate biodegradation. Variations in diamondoid concentration and isomerization ratios might reflect severe biodegradation of oils. The conflicting evidence from biomarker maturity indices and diamondoid concentrations in oils might result from water washing, but the effect of water washing is insignificant on diamondoid isomerization and concentration ratios, unless severe water washing has occurred. Phase fractionation caused by gas washing alters both the absolute concentration and relative contents of diamondoids. Diamondoid concentrations in condensates related to gas washing are significantly lower than in those formed by thermal cracking. Therefore, diamondoid absolute concentration can be used to differentiate between phase fractionation and thermal cracking origins for condensates. Mixed oils can be identified from discrepancies between diamondoid concentrations and other parameters (e.g., API and T/(T + P) values). In summary, diamondoid indices can be used to identify the different types and intensity of reservoir alteration in oils.

CRediT authorship contribution statement

Wenmin Jiang: Investigation, Data curation, Writing - original draft, Validation. **Yun Li:** Conceptualization, Writing - review & editing, Validation. **Yongqiang Xiong:** Methodology, Supervision.

Declaration of competing interest

The authors declare that they have no known competing financial interests or personal relationships that could have appeared to influence the work reported in this paper.

Acknowledgements

This work was supported by the National Natural Science Foundation of China (Grant Nos. 41773034 and 41372138), the National Natural Science Foundation of Guangdong Province (Grant No. 2018B030306006), the Youth Innovation Promotion Association CAS (Grant No. 2018386), and the Self-Research Foundation of the State Key Laboratory of Organic Geochemistry, GIGCAS (Grant No. SKLOG2016-A02). This work is contribution No. IS-2862 from GIGCAS.

Appendix A. Supplementary data

Supplementary data to this article can be found online at https://doi.org/10.1016/j.marpetgeo.2020.104451.

References

Cao, J., Zhang, Y.J., Hu, W.X., Yao, S.P., Wang, X.L., Zhang, Y.Q., Tang, Y., 2005. The Permian hybrid petroleum system in the northwest margin of the Junggar Basin, northwest China. Mar. Petrol. Geol. 22, 331–349.

Cao, J., Yao, S., Jin, Z., Hu, W., Zhang, Y., Wang, X., Zhang, Y., Tang, Y., 2006. Petroleum migration and mixing in the northwestern Junggar Basin (NW China): constraints from oil-bearing fluid inclusion analyses. Org. Geochem. 37, 827–846.

Chang, X.C., Zhao, H.G., He, W.X., Xu, Y.H., Xu, Y.D., Wang, Y., 2018. An improved understanding of the alteration of molecular compositions by severe to extreme biodegradation: a case study from the Carboniferous oils in the eastern Chepaizi Uplift, Junggar Basin, NW China. Energy Fuels 32, 7757–7768.

Chen, J.H., Fu, J.M., Sheng, G.Y., Liu, D.H., Zhang, J.J., 1996. Diamondoid hydrocarbon ratios: novel maturity indices for highly mature crude oils. Org. Geochem. 25, 179–190.

Chen, J.P., Deng, C.P., Liang, D.G., Wang, X.L., Zhong, N.N., Song, F.Q.P., Shi, X., Jin, T., Xiang, S.Z., 2003. Mixed oils derived from multiple source rocks in the Cainan oilfield, Junggar Basin, northwest China. Part II: artificial mixing experiments on typical crude oils and quantitative oil-source correlation. Org. Geochem. 34, 911–930.

Chen, J.P., Wang, X.L., Deng, C.P., Liang, D.G., Zhang, Y.Q., Zhao, Z., Ni, Y.Y., Zhi, D.M., Yang, H.B., Wang, Y.T., 2016a. Geochemical features of source rocks and crude oil in the Junggar Basin, Northwest China. Acta Geol. Sin. 90, 37–67.

Chen, J.P., Wang, X.L., Deng, C.P., Liang, D.G., Zhang, Y.Q., Zhao, Z., Ni, Y.Y., Zhi, D.M., Yang, H.B., Wang, Y.T., 2016b. Oil and gas source, occurrence and petroleum system in the Junggar Basin, northwest China. Acta Geol. Sin. 90, 421–450 (in Chinese with English abstract).

Chen, S.J., Zhan, Y., Lu, J.G., Lu, L.C., Chen, X., Wang, Y., 2010. Cretaceous hydrocarbon formation and migration direction in Well Shinan 31 in the hindland of Junggar Basin. Petrol. Geol. Exp. 32, 382–386 (in Chinese with English abstract).

Chen, T., Hou, D.J., Mi, J.L., He, D.S., Shi, H.S., Zhu, J.Z., 2015. Study on gas washing of crude oils in Baiyun sag. J. Northeast Petrol. Univ. 39, 60–66 (in Chinese with English abstract).

Chen, Z.L., Liu, G.D., Wang, X.L., Gao, G., Xiang, B.L., Ren, J.L., Ma, W.Y., Zhang, Q., 2016c. Origin and mixing of crude oils in Triassic reservoirs of Mahu slope area in Junggar Basin, NW China: implication for control on oil distribution in basin having multiple source rocks. Mar. Petrol. Geol. 78, 373–389.

Cheng, X., Hou, D.J., Xu, C.G., 2018. The effect of biodegradation on adamantanes in reservoired crude oils from the Bohai Bay Basin, China. Org. Geochem. 123, 38–43.

Clayton, J.L., Yang, J., King, J.D., Lillis, P.G., Warden, A., 1997. Geochemistry of oils from the Junggar Basin, northwest China. AAPG (Am. Assoc. Pet. Geol.) Bull. 81, 1926–1944.

Cui, J.W., Wang, T.G., Wang, C.J., Li, M.J., 2012. Quantitative assessment and significance of gas washing of oil in block 9 of the tahe oilfield, Tarim Basin, NW China. Chin. J. Geochem. 31, 165–173.

Curiale, J., Bromley, B., 1996. Migration induced compositional changes in oils and condensates of a single field. Org. Geochem. 24, 1097–1113.

Da, J., Hu, Y., Zhao, M.J., Song, Y., Xiang, B.L., Qin, S.F., 2010. Feature of source rocks and hydrocarbon pooling in the Kelameili gasfield, the Junggar Basin. Oil Gas Geol. 31, 187–192 (in Chinese with English abstract).

Fu, S., Wang, C.S., Tian, J.C., Wu, X.H., 2005. Biodegradation characteristics of the oil from the Luliang oil field of Junggar Basin, China. J. Chengdu Univ. Technol. (Sci. Technol. Ed.) 32, 252–256 (in Chinese with English abstract).

Grice, K., Alexander, R., Kagi, R.I., 2000. Diamondoid hydrocarbon ratios as indicators of biodegradation in Australian crude oils. Org. Geochem. 31, 67–73.

Huang, P., 2017. The Oil-Source Correlation of Crude Oils and Source Rocks from the Northwestern Margin of Junggar Basin [D]. University of Chinese Academy of Sciences.

Jiang, W.M., Li, Y., Xiong, Y.Q., 2019. Source and thermal maturity of crude oils in the Junggar Basin in northwest China determined from the concentration and distribution of diamondoids. Org. Geochem. 128, 149–160.

Lafargue, E., Barker, C., 1988. Effect of water washing on crude oil compositions. AAPG (Am. Assoc. Pet. Geol.) Bull. 72, 263–276.

Larter, S., Mills, N., 1991. Phase-controlled molecular fractionation in migrating petroleum charges. Geol. Soc. London 1, 137–147.

Li, Y., Xiong, Y.Q., Chen, Y., Tang, Y.J., 2014. The effect of evaporation on the concentration and distribution of diamondoids in oils. Org. Geochem. 69, 88–97.

Li, Y., Chen, Y., Xiong, Y.Q., Liang, Q.Y., Fang, C.C., Chen, Y., Wang, X.T., Liao, Z.W., Peng, P.A., 2018. The application of diamondoid indices in the Tarim oils. AAPG (Am. Assoc. Pet. Geol.) Bull. 101, 267–291.

Liang, Q.Y., Xiong, Y.Q., Fang, C.C., Li, Y., 2012. Quantitative analysis of diamondoids in crude oils using gas chromatography - triple quadrupole mass spectrometry. Org. Geochem. 43, 83–91.

Liu, H.J., Zhang, Z.H., Qin, L.M., Zhu, L., Xi, W.J., 2011. Accumulation mechanism of light oils in chepaizi uplift belt of junggar basin. J. China Univ. Petrol. (Ed. Nat. Sci.) 35, 34–40 (in Chinese with English abstract).

Liu, G.D., Chen, Z.L., Wang, X.L., Gao, G., Xiang, B.L., Ren, J.L., Ma, W.Y., 2016. Migration and accumulation of crude oils from Permian lacustrine source rocks to Triassic reservoirs in the Mahu depression of Junggar Basin, NW China: constraints from pyrrolic nitrogen compounds and fluid inclusion analysis. Org. Geochem. 101, 82–98.

Long, H.S., Li, J., Wang, X.L., Wei, L.C., Xie, Z.Y., Liao, J.D., Xiang, C.F., 2014. Effective hydrocarbon kitchen in Kelameili gas field of Junggar Basin and its control on hydrocarbon accumulation. Xinjing Pet. Geol. 35, 500–506 (in Chinese with English abstract).

Losh, S., Cathles, L., Meulbroek, P., 2002. Gas washing of oil along a regional transect, offshore Louisiana. Org. Geochem. 33, 655–663.

Meulbroek, P., Lawrence, C., Whelan, J.K., 1998. Phase fractionation at south island block 330. Org. Geochem. 29, 223–239.

Pan, C.C., Fu, J.M., Sheng, G.Y., Yang, J.Q., 1999. The determination of oil sources and its significance in the central Junggar basin. Acta Pet. Sin. 20, 27–32 (in Chinese with English abstract).

Pan, C.C., Yang, J.Q., Fu, J.M., Sheng, G.Y., 2003. Molecular correlation of free oil and inclusion oil of reservoir rock in the Junggar Basin, China. Org. Geochem. 34, 357–374.

Peters, K.E., Moldowan, J.M., 1993. The Biomarker Guide: Interpreting Molecular Fossils in Petroleum and Ancient Sediments. Prentice Hall, New Jersey.

Peters, K.E., Walters, C.C., Moldowan, J.M., 2005. The Biomarker Guide: Biomarkers and Isotopes in Petroleum Systems and Earth History. Cambridge University Press, Cambridge.

Sarmah, M.K., Raju, S.V., 2016. Biodegradation and water washing effect on gasoline range hydrocarbons and quality of crude oils from HJN and MKM fields of upper Assam Basin, India. J. Geol. Soc. India 87, 327–336.

Schulz, L.K., Wilhelms, A., Rein, E., Steen, A.S., 2001. Application of diamondoids to distinguish source rock facies. Org. Geochem. 32, 365–375.

Shen, Y., Li, M.R., 2008. A discussion on the genesis of light and heavy oil distribution of inverted sequences in the Chepaizi Uplift, the Junggar Basin. Oil Gas Geol. 29, 66–71 (in Chinese with English abstract).

Thompson, K.F.M., 1987. Fractionated aromatic petroleums and the generation of gas-condensates. Org. Geochem. 11, 573–590.

Thompson, K.F.M., 1988. Gas-condensate migration and oil fractionation in deltaic systems. Mar. Petrol. Geol. 5, 237–246.

Thompson, K.F.M., 2010. Aspects of petroleum basin evolution due to gas advection and evaporative fractionation. Org. Geochem. 41, 370–385.

Thompson, K.F.M., 2016. Hybrid gas condensates and the evolution of their volatile light hydrocarbons. Org. Geochem. 93, 32–50.

Wang, Y.T., 1994. Characteristics of heavy oil biodegradation in the northwestern margin of Junggar Basin. Acta Sedimentol. Sin. 12, 81–88 (in Chinese with English abstract).

Wang, S.J., He, L.J., Wang, J.Y., 2001. Thermal regime and petroleum systems in Junggar basin, northwest China. Phys. Earth Planet. In. 126, 237–248.

Wei, Z.B., Moldowan, J.M., Peters, K.E., Wang, Y., Xiang, W., 2007. The abundance and distribution of diamondoids in biodegraded oils from the San Joaquin Valley: implications for biodegradation of diamondoids in petroleum reservoirs. Org. Geochem. 38, 1910–1926.

Xiang, B.L., Zhou, N., Ma, W.Y., Wu, M., Cao, J., 2015. Multiple-stage migration and accumulation of Permian lacustrine mixed oils in the central Junggar Basin (NW China). Mar. Petrol. Geol. 59, 187–201.

Xiang, C.F., Wang, X.L., Wei, L.C., Li, J., Liang, T.C., Liao, J.D., 2016. Origins of the natural gas and its migration and accumulation pathways in the Kelameili gas field. Nat. Gas Geosci. 27, 268–277 (in Chinese with English abstract).

Xiao, F., Liu, L.F., Zhang, Z.H., Wu, K.J., Xu, Z.J., Zhou, C.X., 2014. Conflicting sterane and aromatic maturity parameters in Neogene light oils, eastern Chepaizi High, Junggar Basin, NW China. Org. Geochem. 76, 48–61.

Xiao, Q., He, S., Yang, Z., He, Z., Wang, F., Li, S., Tang, D., 2010. Petroleum secondary migration and accumulation in the central Junggar Basin, northwest China: insights from basin modeling. AAPG (Am. Assoc. Pet. Geol.) Bull. 94, 937–955.

Yang, D.S., Chen, S.J., Li, L., Lu, J.G., 2012. Hydrocarbon origins and their pooling characteristics of the Kelameili Gas Field. Nat. Gas. Ind. 32, 27–31 (in Chinese with English abstract).

Yu, S., Wang, X.L., Xiang, B.L., Liao, J.D., Wang, J., Li, E.T., Yang, Y.H., Cai, Y.L., Zou, Y.R., Pan, C.C., 2014. Organic geochemistry of carboniferous source rocks and their generated oils from the eastern junggar basin, nw China. Org. Geochem. 77, 72–88.

Zhang, D., Huang, D., Li, J., 1988. Biodegraded sequence of Karamay oils and semi-quantitative estimation of their biodegraded degrees in Junggar Basin, China. Org. Geochem. 13, 295–312.

Zhang, B., Huang, L., Wu, Y., Wang, H., Cui, J., 2010a. Quantitative evaluation of crude oil composition changes caused by strong gas washing: a case study of natural gas pool in Kuqa Depression. Earth Sci. Front. 17, 270–279 (in Chinese with English abstract).

Zhang, Z.H., Qin, L.M., Li, W., Wang, C.J., Qiu, N.S., Meng, X.L., Zhang, Z.Y., Yuan, D.S., 2010b. Source and commingling features of light oils from the chepaizi uplift in the junggar basin, northwest China. Chin. J. Geochem. 29, 121–129.

Zhang, Z.H., Liu, H.J., Li, W., Fei, J.J., Xiang, K., Qin, L.M., Xi, W.J., Zhu, L., 2014. Origin and accumulation process of heavy oil in Chepaizi area of Junggar Basin. J. Earth Sci. Environ. 36, 18–32 (in Chinese with English abstract).

Zhang, S.C., 2000. Migration fractionation: an important formation mechanism of condensates and waxy oils. Chin. Sci. Bull. 45, 667–670 (in Chinese with English abstract).

Zou, H.Y., Hao, F., Zhang, Q.B., Chen, B., 2005. History of hydrocarbon-filling and re-migrating in hinterland of the Junggar Basin. Chin. J. Geol. 40, 499–509 (in Chinese with English abstract).